Self-Assembly

DOI: 10.1002/anie.201102342

DNA-Linked Nanoparticle Building Blocks for Programmable Matter**

Jin-Woo Kim, Jeong-Hwan Kim, and Russell Deaton*

Programmable matter is a distributed system of agents that act cooperatively to configure themselves into arbitrary shapes with arbitrary functions.[1] Molecular self-assembled structures containing many nanoparticles are candidates for programmable matter.[1c] Programmability implies that system designers are able to control the properties of assembly products. The system should be able to assemble into arbitrary, anisotropic shapes, like an electronic circuit, with the capability of incorporating different materials at specific locations within the structure. Defects or errors should be minimized, and 3D assembly should be possible. In self-assembly, component parts, or building blocks, interact locally to produce a coherent and organized whole.[2] At the molecular level, the interactions are determined by "patches" that react between building blocks. Frequently, the assemblies exhibit collective properties that are distinct from those of their constituent components.[3] These properties often depend upon the shape of the structure. Thus, the difficulty of programmability is really the difficulty of controlling the shape of resulting nanostructures. The ability to program the shape of a final assembly is computationally difficult[4] and subject to frequent errors.[5] Nevertheless, through careful design and implementation of building blocks, desired shapes and properties might be achieved. To maximize programmability (i.e., control), there should be a large number of types of patches available. Otherwise, there is no variety of interactions to assemble complicated shapes. The placement and relative orientation of patches on the surface of the building block should be controlled. Different types of patches should be able to be placed on the same building block to diversify the shapes available. Finally, the chemistry for patch conjugation to the building block should be relatively simple and sustainable, and it should be able to be used with a variety of materials.

Because of its unique molecular recognition properties, structural features, and ease of manipulation, beginning with seminal work by Seeman and Chen,[6] DNA has been considered as a promising material to achieve programmable assembly of nanostructures. Nanoparticle (NP) building blocks with different surface functionalities for DNA linkers have been reported.[7] DNA computing[8a] verified the programmability of DNA-based nanotechnology and, in fact, demonstrated that DNA self-assembly was computation-universal.[8b] DNA programmability has demonstrated the ability to assemble a variety of shapes[1c,6,9] and, when NPs are incorporated, to control the position of NPs in linear, 2D, and 3D assemblies, including those based upon origami techniques.[3,4,7,10] Nevertheless, the rational self-assembly of functional structures with arbitrary shapes in all dimensions and at all scales that can incorporate many different NPs into a variety of final geometries remains difficult to attain.

Herein we present a strategy to control the number, placement, and relative orientation of DNA linkers on the surface of a colloidal NP building block to maximize its programmability and realize enhanced control over the shape and function of final self-assembled structures. Figure 1 shows a schematic illustration of the assembly sequence to produce the DNA-linked colloidal gold NP building blocks (termed nBLOCKs). A measure of control was achieved by the sequential ligand replacement approach[11] and stiff DNA linkers, which were shorter than the persistence length of double-stranded DNA. In the assembly reaction, the electrostatic repulsions and steric hindrances of DNA molecules influence the layout of DNA on a NP. The net charge of DNA at a pH value above its isoelectric point (i.e., $pH \approx 5$) is negative, so it would tend to position on a NP to minimize its mutual electrostatic repulsions, in analogy to the valence shell electron pair repulsion model, thus contributing to the molecular geometry. Also, mutual steric hindrance could be another factor to further constrain the overall geometry, particularly using small NPs.[7a] In our strategy, a Au NP is functionalized by DNA strand by strand: for example, a NP with one DNA strand is the starting material for the second DNA attachment, a NP with two DNA strands is the starting material for the third DNA attachment, etc. (Figure 1; see Figure S1 in the Supporting Information). With this constraint, the position of DNA attachment would be chosen to minimize the electrostatic and steric interactions with existing DNA on the NP, yielding the optimal arrangement of DNA on a NP with up to sixfold symmetry, that is, linear (one and two DNA strands), T-shaped (three DNA strands), square planar (four DNA strands), square pyramidal (five DNA

[*] Prof. J.-W. Kim, Dr. J.-H. Kim
Bio/Nano Technology Laboratory
Department of Biological and Agricultural Engineering and
Institute for Nanoscience and Engineering
University of Arkansas, Fayetteville, AR 72701 (USA)
E-mail: jwkim@uark.edu

Prof. R. Deaton
Department of Computer Science and Computer Engineering
University of Arkansas, Fayetteville, AR 72701 (USA)

[**] This research has been supported in part by National Science Foundation grant number CMMI-0709121 (J.-W.K. and R.D.) and the Arkansas Biosciences Institute (J.-W.K.). We thank Ju Seok Lee for his assistance with DNA sample preparation, Hee-Jeung Kim for her assistance in image processing, and Min Kim for her artwork for the back cover picture.

Supporting information for this article is available on the WWW under http://dx.doi.org/10.1002/anie.201102342.

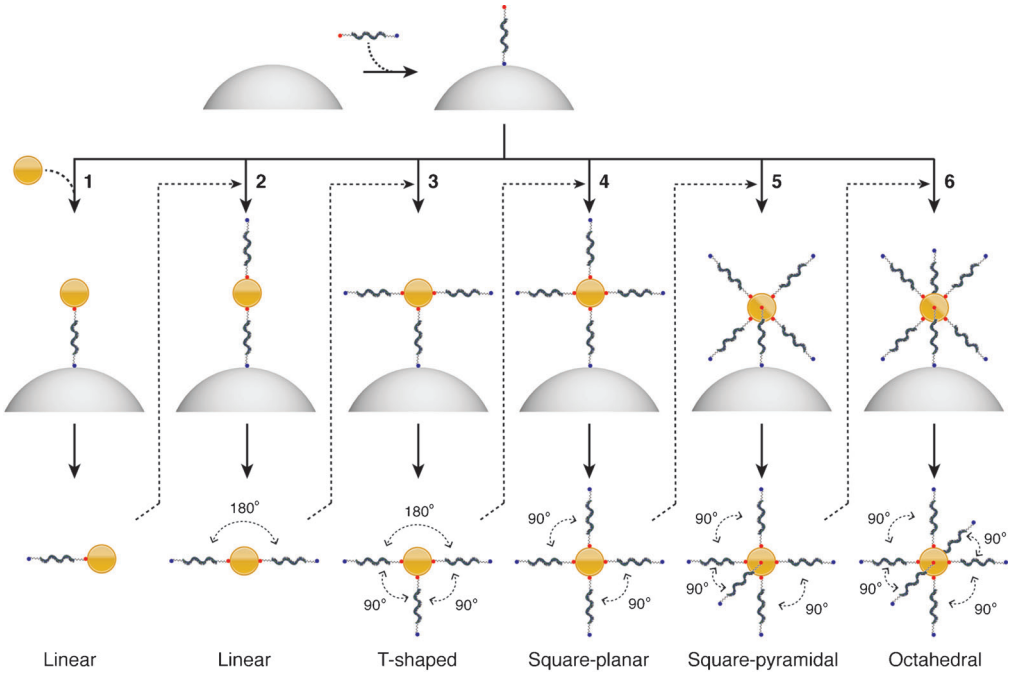

Figure 1. Synthesis of DNA-linked Au NP building blocks (nBLOCKs) with up to sixfold symmetry. Numbers represent the sequences of the aqueous-phase anisotropic sequential ligand replacement strategy. DNA oligonucleotide linker (green curved line) has chemically modified amine (blue dot) and thiol (red dot) ends. Yellow circles are Au NPs co-modified with 4-dimethylaminopyridine (DMAP) and mercaptoethane sulfonic acid (MESA) capping ligands; the gray semicircle is 4-carboxybutyl-functionalized silica gel. DNA is attached to the NP strand by strand. Thus, a NP with one DNA strand is the starting material for the second DNA attachment. The incoming DNA strand maximally segregates from the already attached DNA, producing an angle of approximately 180°. This complex is then used as the starting material for the third DNA attachment. To maximally segregate from the two attached DNA strands, the third strand would attach at an angle of 90°, producing the T-shaped structures. Likewise, attachment of a fourth DNA strand would produce a NP with DNA at 90° angles, that is, square-planar. Subsequent attachments would proceed in this fashion, producing the postulated geometries. See the Experimental Section and Figure S1 in the Supporting Information for details of the experimental design.

strands), and octahedral (six DNA strands, Figure 1; see Figure S1 in the Supporting Information). In the absence of such a constraint (i.e., simultaneous DNA attachment), the arrangement of three, four, and five DNA strands would tend to be trigonal-planar, tetrahedral, and trigonal-bipyramidal, respectively. However, our sequential strand-by-strand attachment strategy would produce different geometries than simultaneous attachment, thus yielding the postulated configurations.

Figure 2a shows the reaction solutions during the first sequence of the DNA functionalization process (see Figure 1 and Figure S1 in the Supporting Information), which was designed based upon the silica-gel-based aqueous-phase anisotropic ligand replacement strategy.[11a] By repeating the process, control over the DNA linker's number, location, and orientation on the NP could be achieved. The functionalization reaction occurred in mild aqueous conditions at ambient temperature, and a reaction sequence could be completed in one hour. Moreover, nonspecific adsorptions and interactions between DNA, Au NPs, and silica gels were very minimal. The rapid, efficient, and mild reaction in aqueous solution can be attributed to the sustainable chemistry of reagents, including Au NP capping ligands, silica gels, and chemically modified DNA linkers (see the Supporting Information, Note 1). Also of note is the excellent aqueous solubility and chemical stability of Au NPs and nBLOCKs during the ligand replacement reactions (Figure 2a). Moreover, no apparent changes in their physical and chemical properties were observed at least for a month when they were stored at 4°C. Furthermore, our aqueous-phase anisotropic functionalization strategy should work for other NPs that have their surface capped with a self-assembled monolayer of polymeric ligands with chemical head groups (i.e., thiol, amine, or phosphine), implying the versatility of our technique.

Ethidium bromide staining agarose gel imaging of nBLOCKs (Figure 2b) revealed not only the association of DNA with nBLOCKs under UV light but also the increase of their molecular weight as the degree of functionalization increased, thus indicating that our method could control the number of DNA strands on a Au NP. Also, as the geometric dimensions of the nBLOCKs increased, their mobility decreased exponentially (i.e., separation of lanes 1 [1D] and 2 [1D] vs. that of lanes 2 [1D] and 3 [2D] vs. that of lanes 4 [2D] and 5 [3D]), thus implying successful assembly of the geometric configurations as postulated. Moreover, the relatively well-defined bands with minimal background (although the smearing became slightly apparent for the more complex and bulkier 3D nBLOCKs (particularly lane 6 with six DNA strands)) imply high-purity concentrations of nBLOCKs and their outstanding solubility and monodispersity in water. Incorporation of a separation process, such as gel extraction, size-exclusion chromatography, etc., would even further improve the product purity. The results of optical spectral analyses (Figure 2c,d) were in good agreement with those of the gel electrophoresis. All nBLOCKs exhibit peaks at both approximately 260 nm for DNA and 530 nm for Au NPs, thus indicating successful functionalization of DNA to the Au NP surface. Using the absorption of Au NPs at 530 nm as reference, we calculated the yield of nBLOCKs at each sequence to be in the range of 92–95% (Figure 2c, inset; see the Supporting Information, Note 2), thus verifying the high

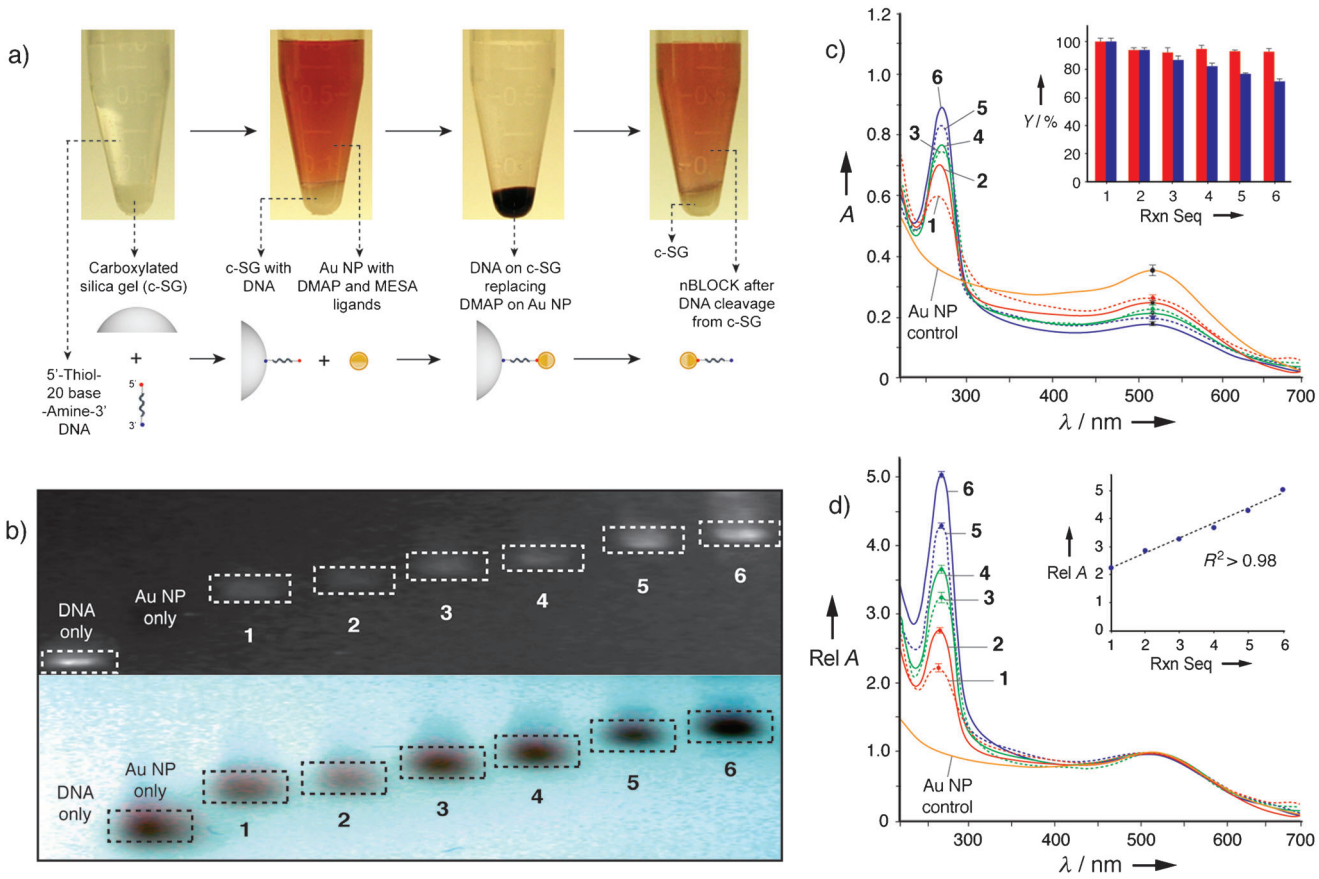

Figure 2. Analyses of the nBLOCK assembly process. a) Reaction solutions with schematic depictions showing each step of the first sequence of the aqueous-phase ligand replacement method. Multiligand functionalization is achieved by repeating the sequence. b) Agarose gel images of nBLOCKs under UV (top) and visible (bottom) light. Numbers represent: 1–6, nBLOCKs with one to six DNA strands (D1; see Table S1 in the Supporting Information). c) Optical spectra of nBLOCKs. Inset: the estimated yield at each sequence (red) and overall yield after the sequence (blue). d) Normalized optical spectra of nBLOCKs. Inset: DNA concentration profile during the ligand replacement reaction sequences. Numbers in (c) and (d) represent the sequences of the ligand replacement method. Error bars represent the standard deviation in five measurements.

efficiency of our aqueous-phase ligand replacement method. Also, the relative optical spectra at a fixed concentration of Au NPs (Figure 2d) showed almost linear increase of DNA absorption intensity after each functionalization sequence, clearly confirming our method's capability to control the number of DNA strands on a Au NP.

To assess the molecular geometry of the functionalized DNA in nBLOCKs, a Au NP with one complementary DNA sequence was hybridized with each nBLOCK. Transmission electron microscopy (TEM) image analyses revealed that the molecular geometry of NPs in the self-assembled structures was diatomic for nBLOCK with one DNA strand, linear for two DNA strands, T-shaped for three DNA strands, square-planar for four DNA strands, square-pyramidal for five DNA strands, and octahedral for six DNA strands (Figure 3). The average interparticle distances ((9.7 ± 3.94) nm) of 1D and 2D structures were in agreement with the calculated interparticle distance (ca. 11 nm). The angles between three particles across two DNA linkages averaged (173.9 ± 9.88)° for the linear configurations (Figure 3b) and (84.9 ± 8.68)° and (173.2 ± 10.01)° for T-shaped and square-planar configurations, respectively (Figure 3c,d; see the Supporting Information, Note 3), thus suggesting the excellent control of our strategy over the orientation and spatial arrangement of DNA linkers. We could not assess the interparticle distances and angles for 3D structures owing to technical limitations of evaluating TEM images of 3D structures; however, TEM images with accompanying schematic illustrations (Figure 3e,f and Figure 4) provide evidence for the formation of 3D square-pyramidal and octahedral geometries. Other geometries are visible in the TEM images. These could be caused by flexibility in the DNA linking NPs or by depth effects producing foreshortening of the structure's geometry. Nevertheless, given the strand-by-strand functionalization method, the anchor-point of a new DNA strand on a NP in each step should be at a 90° or 180° angle to that of the adjacent DNA strand existing on the NP to achieve maximal segregation for minimal electrostatic and steric interactions. Thus, no other physical mechanism may be feasible for producing alternative geometries of DNA on a NP, such as those for the simultaneous DNA attachment as mentioned above. However, detailed structural geometries remain to be further interrogated using more sophisticated analyses, such as small-angle X-ray scattering.

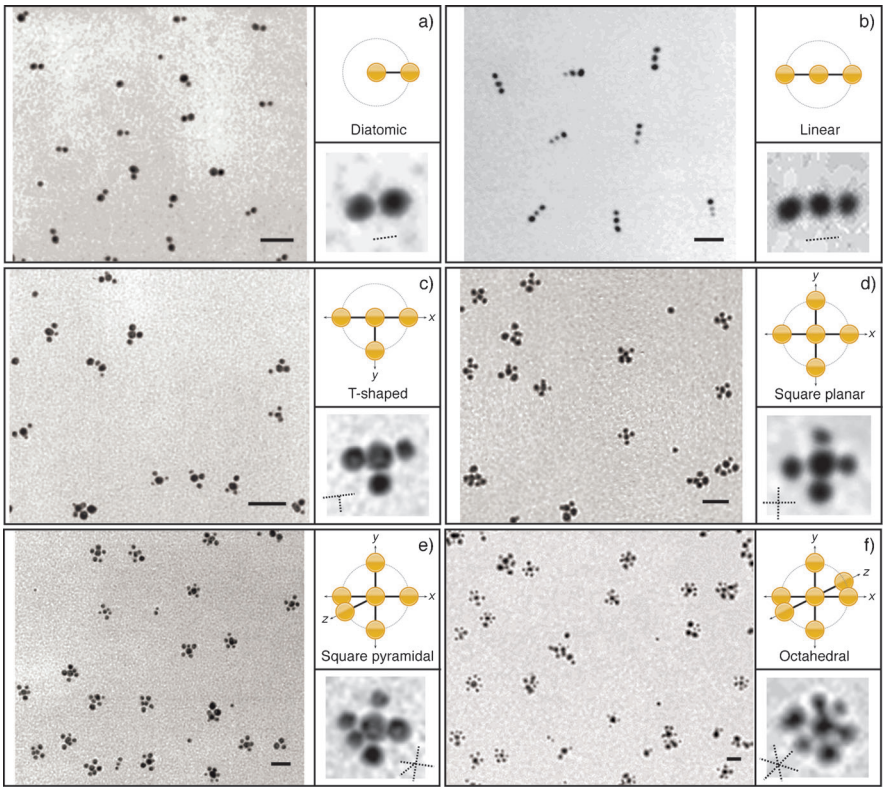

Figure 3. Molecular geometry of nBLOCK visualized by TEM and its schematic representation. Each nBLOCK was hybridized with a monofunctionalized nBLOCK with a single complementary DNA oligonucleotide (D1^c; see Table S1 in the Supporting Information). Left panels: TEM images of the self-assembled structures. Bottom right panels: magnified TEM images. Top right panels: schematic illustration of the assembled structures, showing nBLOCK up to sixfold symmetry (all *x*, *y*, and *z* directions). In the schematic depictions, the solid lines represent double-stranded DNA and the gray dotted circles the 2D plane. Scale bars represent 20 nm.

In summary, we have demonstrated a strategy to place DNA linkers on a NP at specific angles to each other and to produce NP building blocks with well-defined arrangements of DNA in all dimensions. The specific number and orientation of DNA strands on NPs allow greater control over the ultimate shape of nanostructures, thus making DNA-guided self-assembly process more reproducible and scalable and allowing the assembly of complex hybrid nanoscale architectures at all scales and in all dimensions. The reaction was not only highly sustainable, as it is in the aqueous phase, but it is also highly efficient and easy to implement. Our strategy also invites generalization. The spacing between particles could be tuned by the length of the DNA strands, and the overall geometry of DNA on a NP could be influenced by the extent of electrostatic repulsion and steric hindrance between DNA strands. Different DNA linkers could be placed at different locations on NPs, thus increasing the size and complexity of the nanostructure to be assembled. The potential errors could be minimized through appropriate DNA sequence design.[12] Finally, our strategy has promise to be generalized to other types of NPs. Therefore, it has the potential to produce NP building blocks with the desired properties in a programmable matter, that is, arbitrary, anisotropic shapes, including in three dimensions, of structures with specific, desired functions, and precision difficult to achieve with existing methods. The manipulation of matter in such a controlled way at the molecular scale would enable a wide range of significant applications, from tissue engineering to new types of electronics, and a variety of new materials with interesting properties, from optical and electrical to structural.

Experimental Section

Synthesis of water-soluble Au NPs: Water-soluble dimethylaminopyridine (DMAP) monolayer-protected Au NPs were purchased from Sigma–Aldrich. The reported ligand-exchange method[11a] was used to produce a robust and stable mixed monolayer with mercaptoethane sulfonic acid (MESA) ligands to enhance their chemical stability during functionalization with DNA. The final concentration of the resultant Au NPs co-modified with DMAP and MESA ligands was estimated to be 6 μM in water by UV/Vis/NIR spectral analysis ($\varepsilon \approx 1\times10^6\,\text{M}^{-1}\,\text{cm}^{-1}$). The Au NPs showed excellent solubility in biological buffer solutions (Figure 2a) and a net negative charge according to the gel electrophoresis results (Figure 2b). As estimated with TEM, the ligand-capped Au NPs were well-dispersed with an average diameter of (2.83 ± 0.47 nm, Figure S2 in the Supporting Information).

Synthesis of DNA-linked nBLOCKs: A DNA oligonucleotide (D1) and its complementary sequence (D1^c) with chemically modified 3′ and 5′ ends were designed and purchased from Integrated DNA Technologies. The oligonucleotide sequences are summarized in Table S1 in the Supporting Information. The 4-carboxybutyl-functionalized silica gels (c-SGs) were purchased from Silicycle. Our DNA functionalization technique (Figure 1 and Figure 2a; see Figure S1 in the Supporting Information) started with electrostatically binding the positively charged amine end of the DNA to the negatively charged surfaces of c-SGs. Briefly, the reaction mixture consisted of DNA (3.97 mM) and c-SGs (50 mg) in boric acid buffer (1 mL, 10 mM, pH 7.4) and was incubated overnight with gentle mixing. The DNA-modified c-SGs (DNA–c-SGs) were then washed three times by centrifugation and resuspension with 10 mM phosphate buffer with 10 mM NaCl (pH 7.4). As estimated by UV/Vis/NIR spectrophotometry, the loading yield of DNA linkers on c-SG beads was approximately 90%. For the ligand replacement reaction, the thiol group at the 5′-end of DNA bound to c-SGs was activated by adding dithiothreitol (400 μL, 50 mM) with 2 vol% triethylamine to DNA–c-SG solution (1 mL) and incubating for 10 min with vigorous agitation. The activated DNA–c-SGs were rinsed three times by centrifugation and resuspension with the phosphate buffer, resuspending to 1 mL phosphate buffer. The ligand replacement reaction was continued by adding Au NP solution (1.2 μM) to the activated DNA–c-SG solution (1 mL) and incubating for 1 h with gentle shaking. This procedure allowed DNA on silica gels to replace a short DMAP ligand on the Au NPs, making the color of c-SGs change from white to dark red (Figure 2a). The Au NP–DNA–c-SGs were rinsed three times by centrifugation and resuspension with the boric acid buffer, resuspending to 1 mL ethanol. Finally, the electrostatically bound DNA was released from c-SGs by adding 0.5 vol% trifluoroacetic acid with gentle mixing for approximately 30 s. This step

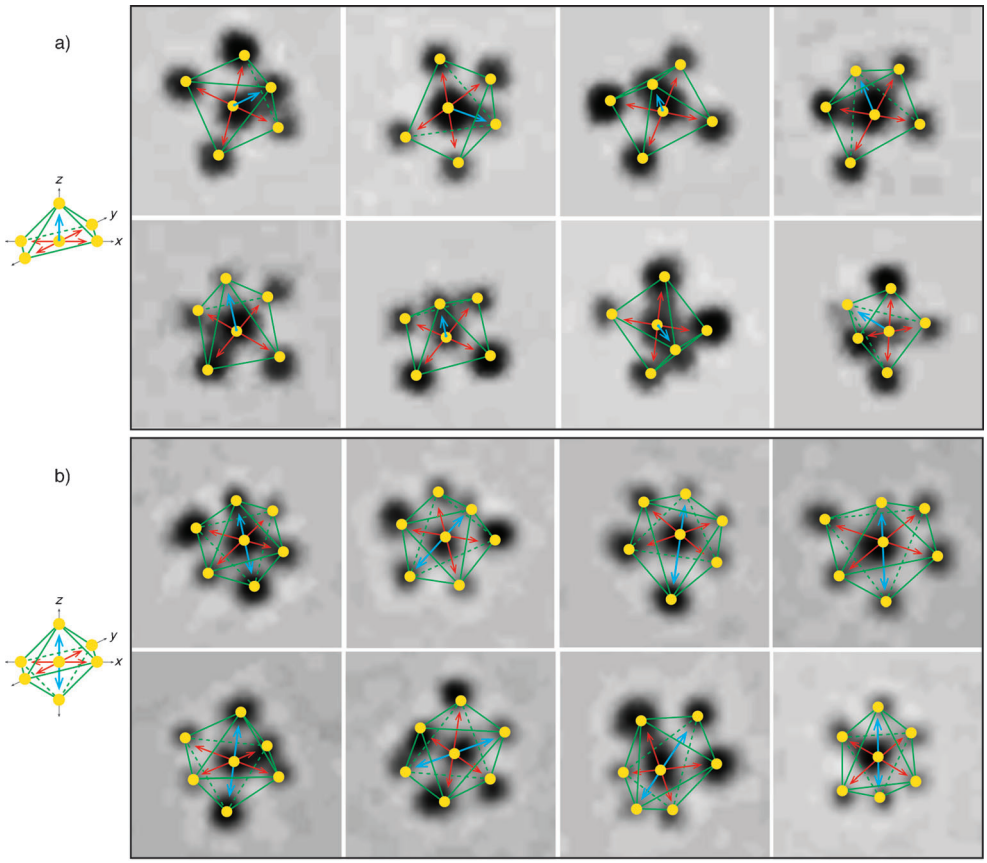

Figure 4. TEM images and the geometric interpretation of 3D nBLOCKs. a) 3D square-pyramidal and b) 3D octahedral nBLOCKs after hybridization with a monofunctionalized nBLOCK with a single complementary DNA oligonucleotide. Lines represent geometric trends of the self-assembled structures, providing evidence for the formation of the corresponding 3D geometries.

effectively cleaved DNA from c-SGs, turning solution red (Figure 2a). The resultant monofunctionalized Au NP nBLOCKs with one DNA strand were rinsed three times by centrifugation and resuspension with 1 mL water and resuspended in 1 mL 10 mM tris(hydroxymethyl)aminomethane (Tris)-HCl buffer (pH 7) for the next sequence of functionalization. For the second functionalization sequence, we repeated the above steps with a modification. The DNA–c-SGs were suspended in the Tris-HCl buffer instead of the phosphate buffer to block free (i.e., unoccupied) carboxy groups on c-SGs, alleviating the undesirable nonspecific interactions between carboxy groups on c-SGs and amine groups of DNA in nBLOCKs. By repeating the process with this change, we could achieve the control over DNA linker's number, location, and orientation on the NP in all three dimensions. The DNA-linked nBLOCKs synthesized in this study include Au NPs with one to six D1 strands and those with one $D1^c$ strand.

Assessment of nBLOCKs: The DNA-linked nBLOCKs were concentrated ten times by centrifugation and resuspension with the Tris-HCl buffer and analyzed using 2% agarose gel electrophoresis. The gel was examined under white light and UV light after staining with ethidium bromide (Figure 2b). The optical absorption spectra of nBLOCKs were examined using a DU-800 UV/Vis/NIR spectrophotometer (Beckman Coulter, Figure 2c). The UV/Vis/NIR spectra were normalized to the absorption of Au NPs at approximately 530 nm in the wavelength range of 230 and 700 nm (Figure 2d). Additionally, each of the six D1-linked nBLOCKs was hybridized with Au NPs with one $D1^c$ linker to assess their molecular geometry. For the hybridization reactions, equal volumes of solutions of D1-linked nBLOCKs and Au NPs with $D1^c$ in the Tris-HCl buffer were mixed and incubated for 1 h at 25 °C. The physical characteristics of the self-assembled structures were assessed with TEM (Supplementary Methods).

Received: April 5, 2011
Revised: June 7, 2011
Published online: September 2, 2011

Keywords: DNA · nanoparticles · nanotechnology · programmable matter · self-assembly

[1] a) T. Toffoli, N. Margolus, *Physica D* **1991**, *47*, 263–272; b) C. A. Mirkin, R. L. Letsinger, R. C. Mucic, J. J. Storho, *Nature* **1996**, *382*, 607–609; c) E. Winfree, F. Liu, L. A. Wenzler, N. C. Seeman, *Nature* **1998**, *394*, 539–544.

[2] G. M. Whitesides, B. Grzybowski, *Science* **2002**, *295*, 2418–2421.

[3] M. R. Jones, R. J. Macfarlane, B. Lee, J. Zhang, K. L. Young, A. J. Senesi, C. A. Mirkin, *Nat. Mater.* **2010**, *9*, 913–917.

[4] Y. Y. Pinto, J. D. Le, N. C. Seeman, K. Musier-Forsyth, T. A. Taton, R. A. Kiehl, *Nano Lett.* **2005**, *5*, 2399–2402; Z. Y. Tang, N. A. Kotov, *Adv. Mater.* **2005**, *17*, 951–962; H. T. Maune, S. Han, R. D. Barish, M. Bockrath, W. A. Goddard III, P. W. K. Rothemund, E. Winfree, *Nat. Nanotechnol.* **2010**, *5*, 61–66; L. Adleman, Q. Cheng, A. Goel, M.-D. Huang, D. Kempe, P. M. de Espanes, P. W. K. Rothemund in *Proc. 34th ACM symposium on Theory of Computing (STOC2002)*, ACM Press, New York, **2002**, 23–32; E. Winfree, P. W. K. Rothemund in *Proc. 32nd ACM symposium on Theory of Computing (STOC2000)*, ACM Press, New York, **2000**, 459–468.

[5] R. Schulman, E. Winfree, *SIAM J. Comput.* **2009**, *39*, 1581–1616; R. Deaton, M. Garzon, R. C. Murphy, J. A. Rose, D. R. Franceschetti, S. E. Stevens, Jr., *Phys. Rev. Lett.* **1998**, *80*, 417–420.

[6] J. Chen, N. C. Seeman, *Nature* **1991**, *350*, 631–633.

[7] a) C. J. Ackerson, M. T. Sykes, R. D. Kornberg, *Proc. Natl. Acad. Sci. USA* **2005**, *102*, 13383–13385; b) K. Suzuki, K. Hosokawa, M. Maeda, *J. Am. Chem. Soc.* **2009**, *131*, 7518–7519; c) S. Y. Park, A. K. R. Lytton-Jean, B. Lee, S. Weigand, G. C. Schatz, C. A. Mirkin, *Nature* **2008**, *451*, 553–556; d) D. N. Nykypanchuk, M. M. Maye, D. van der Lelie, O. Gang, *Nature* **2008**, *451*, 549–552.

[8] a) L. M. Adleman, *Science* **1994**, *266*, 1021–1024; b) E. Winfree, X. Yang, N. C. Seeman, *In DNA Based Computers*, Vol. 44 of DIMACS (Eds: L. F. Landweber E. B. Baum), AMS press, Providence, Rhode Island, **1998**, 191–213.

[9] P. W. K. Rothemund, *Nature* **2006**, *440*, 297 – 302; S. M. Douglas, H. Dietz, T. Liedl, B. Hogberg, F. Graf, W. M. Shih, *Nature* **2009**, *459*, 414 – 418.

[10] F. A. Aldaye, A. L. Palmer, H. F. Sleiman, *Science* **2008**, *321*, 1795 – 1799; J. Sharma, R. Chhabra, C. S. Andersen, K. V. Gothelf, H. Yan, Y. Liu, *J. Am. Chem. Soc.* **2008**, *130*, 7820 – 7821; R. J. Macfarlane, M. R. Jones, A. J. Senesi, K. L. Young, B. Lee, J. Wu, C. A. Mirkin, *Angew. Chem.* **2010**, *122*, 4693 – 4696; *Angew. Chem. Int. Ed.* **2010**, *49*, 4589 – 4592; A. M. Hung, C. M. Micheel, L. D. Bozano, L. W. Osterbur, G. M. Wallraff, J. N. Cha, *Nat. Nanotechnol.* **2010**, *5*, 121 – 126; B. Ding, Z. Deng, H. Yan, S. Cabrini, R. N. Zuckermann, J. Bokor, *J. Am. Chem. Soc.* **2010**, *132*, 3248 – 3249; Z. Zhao, E. L. Jacovetty, Y. Liu, H. Yan, *Angew. Chem.* **2011**, *123*, 2089 – 2092; *Angew. Chem. Int. Ed.* **2011**, *50*, 2041 – 2044.

[11] a) J.-H. Kim, J.-W. Kim, *Langmuir* **2010**, *26*, 18634 – 18638; b) J.-H. Kim, J.-W. Kim, *Langmuir* **2008**, *24*, 5667 – 5671.

[12] W. Yu, J. S. Lee, C. Johnson, J.-W. Kim, R. Deaton, *IEEE Trans. Nanobioscience* **2010**, *9*, 38 – 43; J.-W. Kim, D. P. Carpenter, R. Deaton, *Nanomedicine* **2005**, *1*, 220 – 230; R. Deaton, J.-W. Kim, J. Chen, *Appl. Phys. Lett.* **2003**, *82*, 1305 – 1307.

